

HYDRODYNAMIC EXPERIMENTS FOR MERCURY FLOWING IN ELECTRICALLY CONDUCTING
 AND NON-CONDUCTING PIPES AND BENDS IN A MAGNETIC FIELD

D.R.H. BEATTIE

Australian Nuclear Science and Technology Organisation
 Private Mail Bag 1, Menai, NSW 2234
 AUSTRALIA

ABSTRACT

High Reynolds number pressure losses have been measured for mercury flows in straight pipes and 180° bends in a magnetic field. Flow was normal to the field except for some bends arranged parallel and at 45° to the field. Experiments covered various diameters and conducting as well as non-conducting walls. In the case of non-conducting channels, velocity profiles normal to the field were obtained near the entrance to and exit from the magnet and immediately downstream of the bends.

INTRODUCTION

Liquid metals are attractive as a choice of fusion reactor coolant but suffer the disadvantage of large pressure drops induced by the electrically conducting fluid crossing lines of the magnetic field required to contain the plasma.

As part of a study of the ROTAMAK fusion reactor concept (Durance et al 1987), mercury flow magnetohydrodynamic (MHD) experiments were performed in electrically conducting and non-conducting tubes and 180° bends. Although turbulence is inhibited in MHD flows, interest was in conditions not normally studied where residual turbulence effects might exist. The experiments reported here extend the range of available data (see eg the review of Lielausis 1975). They complement a related analytic study of MHD flows parallel to a magnetic field (Beattie 1989).

EXPERIMENTAL

Nine different U-tube test sections of two straight pipes connected by a 180° bend were used (Table 1). The first five were of copper to ensure good electric contact with the mercury; the other four were of plastic. The flow loop was capable of 4 l/s (55 kg/s) of mercury. The U-tube sections were placed in the 152 mm gap between the two 3.05 m dia polefaces of a

homopolar generator magnet at ANU. Field strengths were remarkably uniform between the polefaces of the magnet. Field strengths beyond the polefaces are shown in fig 1. Flows were normal to the field except in the bend region of four of the test sections (Table 1).

Measurements were made of straight pipe and bend pressure drops, and, for the non-conducting sections, of velocity profiles in the plane normal to the field in the straight pipe sections near the entrance to and exit from the magnet and also immediately downstream of the bend. Local velocities were inferred from voltage differences between consecutive wires of rakes of wires inserted into the flow. Simple manometers were used with the non-conducting sections. The larger pressure drops with the conducting sections (up to 1.5 MPa) necessitated pressure transducers and hence isolating diaphragms in the lines to prevent damage by mercury. Mercury temperatures were about 50°C and were measured with a thermocouple. Flowrates were determined with an electromagnetic flowmeter which required calibration runs to allow for the effect of the field beyond the polefaces on the calibration.

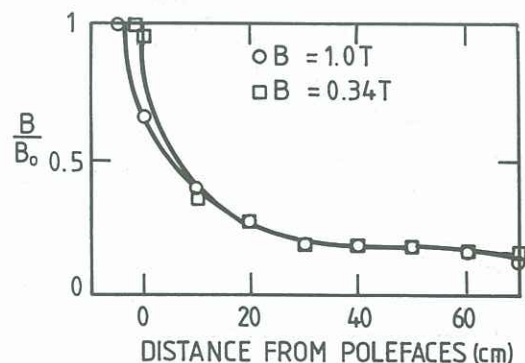


Figure 1 Fringe field of magnet

TABLE 1: Test section details

Test section number	1	2	3	4	5	6	7	8	9
Test section diameter, (mm)	22.1	22.1	22.1	47.6	72.1	22.8	22.8	22.8	50.3
Angle between bend plane and field, (°)	90	45	0	90	90	90	45	0	90
Wall/flow conductance ratio C	7.34	7.34	7.34	3.42	2.82	0	0	0	0
Bend radius, (mm)	27.0	27.0	27.0	80.0	115	39.5	39.5	39.5	80.0
(Bend radius)/(Tube diameter)	1.22	1.22	1.22	1.68	1.59	1.73	1.73	1.73	1.68

RESULTS

Experiments for all test sections were mainly with Reynolds numbers between 10^5 and 10^6 , and with magnetic field strengths between 0.4 and 1.0 T.

Conducting Wall Pressure Drops

In the absence of a magnetic field, straight pipe pressure drops were consistent with standard friction factors for drawn tubing. Bend losses were consistent with equations given by Idelchik (1966) except for the 22.1 mm sections, which had somewhat larger coefficients, perhaps caused by the joins between the bends and straight pipes. For the purposes of this paper, bend losses are incorporated into an effective friction factor

$$f = (P_2 - P_1)D / (2LG\langle u \rangle) \quad 1$$

covering both straight pipes and bends, and the subscript "nf" will refer to values in the absence of a field.

There was no evidence of any additional pressure drop associated with abrupt variations of the field near the magnet entrance. This may be because the fringe field beyond the magnet is more extensive than those of other magnets (all much smaller) discussed in the literature.

Representative friction factors are shown in figs 2-4 as a function of the interaction parameter I . (Average friction factor data involving the magnet's fringe field are plotted against average interaction parameters. This assumes friction factors are unaffected by field gradients, an assumption supported by the present data). Many data are close to the semi-empirical equation of Hoffman and

Carlson (1971) which allows for steep near-wall velocity gradients induced by the field;

$$f_{lmhd} = 1.3 IC / (1+C) \quad 2$$

(the subscripts indicate developed laminar MHD flows), with discrepancies occurring with some flows at low interaction parameters and for some bend data at high interaction parameters.

Apart from the bend data for test section 2 (bend at 45° to the field), low interaction parameter exceptions to equation 2 in figs 2 and 4 are close to

$$f = f_{lmhd} + f_{nr}, \quad 3$$

which has equation 2 as an asymptote since $f_{nr} \ll f_{lmhd}$ at high values of I . Thus, the pressure drop is simply the sum of values for no field and for developed laminar MHD flow. (The bend data are above the pipe data since bend losses are incorporated into f_{nr} for bends).

The presence of f_{nr} suggests the existence of Reynolds stresses. The data indicate that these may persist to an extent not expected from extrapolating our current understanding of magnetic suppression of turbulence within insulated ducts. (Previous examinations have not addressed the role of turbulence in MHD flows in conducting pipes, presumably because of the large pressure drops inherent in any related experiments). Moreover, the effect of these stresses on MHD wall friction is more readily described for conducting walls (equation 3) than for non-conducting walls.

The role of entry length into the field can be gauged by comparing fig 2 data (upstream straight pipes and bends near the magnet entrance, ie short entry

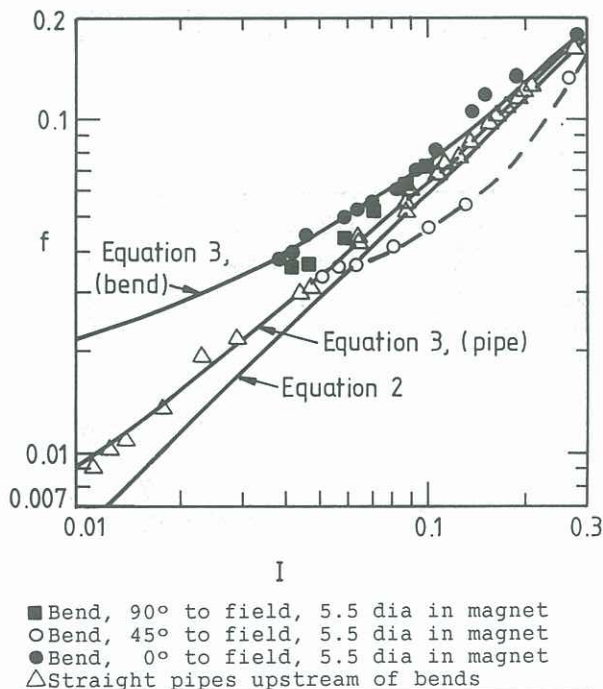


Figure 2 0.4 T friction factors for 22.1 mm sections with short magnetic entrance lengths

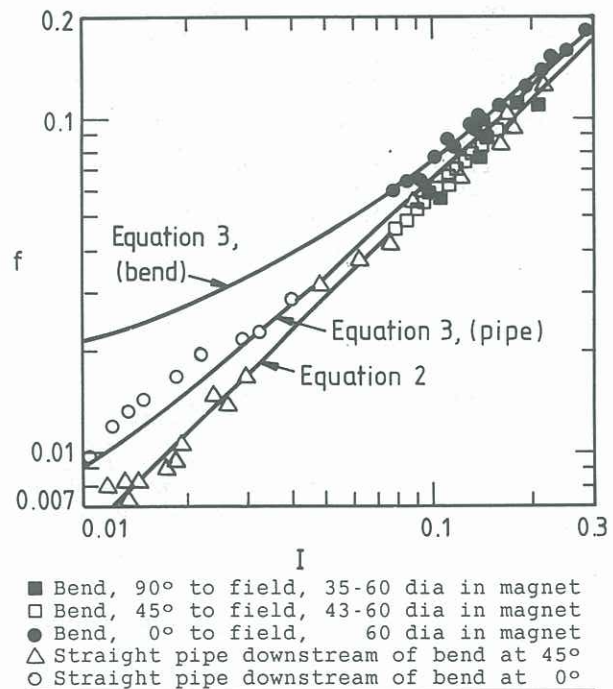


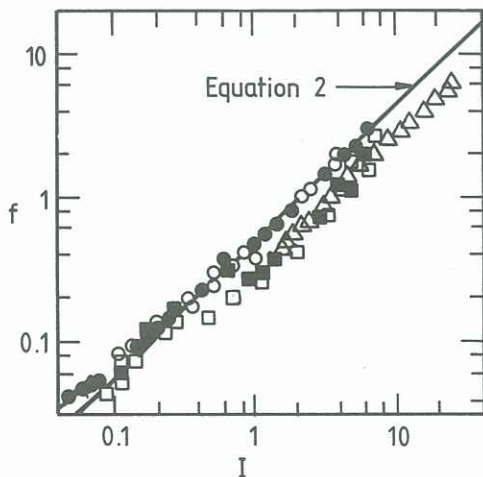
Figure 3 0.4 T friction factors for 22.1 mm sections with long magnetic entrance lengths

lengths) with those of fig 3 (downstream pipes and bends further into the field). Data in fig 3 were obtained with the complete flow circuit in significant magnetic field (including fringe field). The three pressure tappings for the bend and downstream pipe for these data were 102, 113, and 157 dia from a bend near the pump exit. Despite this increased length of field, data from test section 3 are unaltered. Data from the other test sections, however, revert to the laminar flow equation, equation 2, even for shorter entry lengths. Thus, for the conditions examined, a magnetic field by itself is insufficient to suppress Reynolds stresses, but suppression may be achieved with a magnetic field in conjunction with an appropriately oriented bend.

At higher interaction parameters, equations 2 and 3 become indistinguishable, and most data collected here are described by either. Exceptions occur with some bend data at the higher field strengths of these experiments (1T), and are shown in fig 3. Some of the friction factors overpredicted by equation 2 are associated with downstream friction factors slightly greater than given by equation 2, suggesting that the discrepancies are perhaps due to bend effects extending to the pressure tapping downstream of the bend at these larger field strengths. A repositioning of this may yield closer agreement with equation 2.

Non-conducting Duct Pressure Drops and Velocity Profiles

Pressure drop interpretation was complicated by crud- possibly amalgam products from the experiments with the copper sections- migrating to the manometer lines and continually altering levels of the lines for zero flows. The data do, however, strongly suggest that pressure drops were unaltered by the applied field. The height of mercury in the manometer lines did not alter with fixed flow and varying field up to 1.5T.



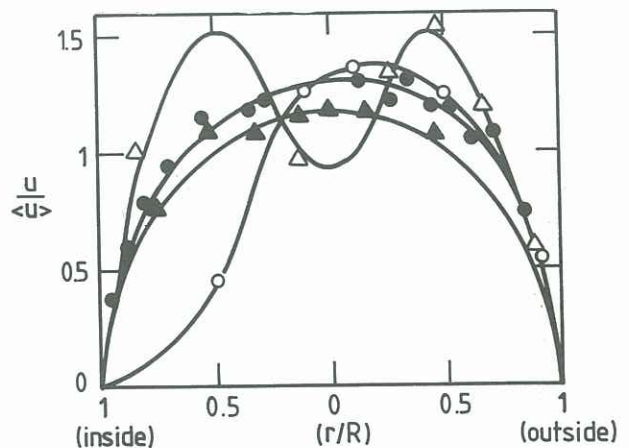
■ 22.1 mm tube bend, 90° to field
 □ 22.1 mm tube bend, 45° to field
 ● 22.1 mm tube bend, 0° to field
 ○ 50.3 mm tube bend, 90° to field
 △ 72.1 mm tube bend, 90° to field
 Figure 4 Friction factor for bends

On the basis of published data (Lielausis 1975), most of our data at lower Reynolds numbers should be unaffected by the field, but a 20-30% effect (not observed) should exist at our higher Reynolds numbers (up to 10⁶).

Velocity profile data were complicated by mercury not wetting the probe tips in the early runs, and damage to the probes caused by the flow in the later runs. Representative velocity profiles are shown in figure 5. In considering these profiles it should be noted that the profiles are not expected to be symmetric; profiles parallel to the field should differ, even for straight pipe flow. The 50 mm straight pipe data are for conditions where complete laminarisation of the flow is expected. The data are well described by the theoretical profile of Shercliff (1956). Downstream of the bend, the 50 mm data of fig 5 show some asymmetry caused by the bend. Bend effects were stronger for the 23 mm sections; moreover, bend orientation appears to play a significant role. The data for the bend parallel to the field show evidence of recirculating flow on the inside, but the profile for the bend 45° to the field is very different, despite otherwise similar flow conditions. The double peak is better confirmed in other profiles of this section; the particular profile shown was chosen because flow conditions were similar to those for the profile shown from test section 3. A double peak often occurs with MHD flows and is associated with electric currents in the direction of flow being induced by flow redistribution. The peaks of the present double-peaked profiles are further from the wall than others reported in the literature, possibly reflecting higher turbulence levels in our high Reynolds number runs.

CONCLUDING DISCUSSION

The liquid metal MHD experiments reported here considerably extend the range of experimental data on pressure drop and velocity profile. They suggest that magnetic fields may not necessarily



D (mm)	Location	Bend/field angle	Re	Ha
▲	50.3 Inlet	n.a.	7.5E4	1140
●	50.3 Downstream	90°	7.2E5	1140
△	22.8 of bend	45°	5.5E5	300
○	22.8 of bend	0°	5.0E5	317

Figure 5 Representative velocity profiles

inhibit turbulence to the extent usually considered, and that bends influence MHD flows in a complex manner. A simple friction factor equation has been proposed for MHD flows with residual turbulence in conducting straight pipes and bends.

REFERENCES

BEATTIE, D. R. H. (1989) Heat transfer in liquid metals flowing in pipes parallel to magnetic fields. p283, Proc 4th Australasian Conf Heat and Mass Transfer

DURANCE, G., HOGG, G. R., TENDYS, J. and WATTERSON, P. A. (1987) Studies of equilibrium in the AEC ROTAMAK. Plasma Physics and Controlled Fusion 29(2) 227

HOFFMAN, M. A. and CARLSON, G. A. (1971) Calculation techniques for estimating the pressure losses for conducting fluid flows in magnetic fields. UCRL report 51010

IDELCHIK, I. E. (1966) Handbook of hydraulic resistance, coefficients of local resistance and of friction. Report AEC-TR-6630

LIELAUSIS, O. (1975) Liquid-metal magnetohydrodynamics. Atomic Energy Review 13, 527

SHERCLIFF, J. A. (1956) The flow of conducting fluids in circular pipes under transverse magnetic fields. J Fluid Mech 1, 644.

NOTATION

B magnetic field strength
B₀ field strength within magnet
c fluid conductivity
c_w wall conductivity
C conductance ratio, c_wt_w/(cR)
d density
D diameter
f generalised friction factor, equation 2
G mass flux
Ha Hartman number, DB(c/v)^{0.5}
I interaction parameter, B²c/(d<u>)
L distance between pressure tappings
P pressure
r radial position
R tube radius
R_b bend radius
Re Reynolds number, d<u>D/v
t_w pipe wall thickness
u local velocity
<u>average velocity
v viscosity

ACKNOWLEDGMENTS

Acknowledgments are due to ANU for making their magnet available; to A Spencer, R J Blevins, M Bloom, D S Faggotter, D Nolan and P R O'Callaghan for their role in designing and constructing the loop and assisting with data collection; to R Marshall (ANU) for liaising with ANSTO and for his role in developing the velocity probes; and to T E Clare for testing the strength of amalgamated copper.